

QCD sum rule analysis of the charmonium system: The charm quark mass

M. Eidemüller* and M. Jamin ^a

^a *Institut für Theoretische Physik, Universität Heidelberg,
Philosophenweg 16, 69120 Heidelberg, Germany*

In this work, the charm quark mass is obtained from a QCD sum rule analysis of the charmonium system. In our investigation we include results from non-relativistic QCD at next-to-next-to-leading order. Using the pole mass scheme, we obtain a value of $M_c = 1.70 \pm 0.13$ GeV for the charm pole mass. The introduction of a potential-subtracted mass leads to an improved scale dependence. The running $\overline{\text{MS}}$ -mass is then determined to be $m_c(m_c) = 1.23 \pm 0.09$ GeV.

1. Introduction

An essential task within modern particle physics lies in the determination of quark masses which are key parameters of the standard model. In the past, QCD moment sum rule analyses have been successfully applied for extracting the charm and bottom quark masses from experimental data on the charmonium and bottomonium systems respectively [1–3]. The fundamental quantity in these investigations is the vacuum polarisation function $\Pi(q^2)$:

$$\begin{aligned} \Pi_{\mu\nu}(q^2) &= i \int d^4x e^{iqx} \langle T\{j_\mu(x)j_\nu(0)\} \rangle \\ &= (q_\mu q_\nu - g_{\mu\nu}q^2) \Pi(q^2), \end{aligned} \quad (1)$$

where the current is represented by $j_\mu(x) = (\bar{c}\gamma_\mu c)(x)$. Via the optical theorem, the experimental cross section $\sigma(e^+e^- \rightarrow c\bar{c})$ is related to the imaginary part of $\Pi(s)$:

$$R(s) = \frac{1}{Q_c^2} \frac{\sigma(e^+e^- \rightarrow c\bar{c})}{\sigma(e^+e^- \rightarrow \mu^+\mu^-)} = 12\pi \text{Im } \Pi(s + i\epsilon).$$

Using a dispersion relation, we can express the moments by an integral over the velocity $v = \sqrt{1 - 4m^2/s}$:

$$\mathcal{M}_n = \frac{12\pi^2}{n!} \left(4m^2 \frac{d}{ds} \right)^n \Pi(s) \Big|_{s=0} \quad (2)$$

*Talk given at the Euroconference on Quantum Chromodynamics (QCD 2000), Montpellier, July 2000

$$= (4m^2)^n \int_{s_{min}}^{\infty} ds \frac{R(s)}{s^{n+1}} = 2 \int_0^1 dv v(1 - v^2)^{n-1} R(v).$$

The moments can either be calculated theoretically, including perturbation theory, Coulomb resummation and non-perturbative contributions, or can be obtained from experiment. In this way, we can relate the charm quark mass to the hadronic properties of the charmonium system.

A natural choice for the mass appearing in eq. (2) is the pole mass M . In the first part of our numerical analysis, we will use the pole mass scheme to extract the charm pole mass. However, as the pole mass suffers from renormalon ambiguities [4], it can only be determined up to corrections of order Λ_{QCD} . In the second part of our analysis we shall therefore use the recently introduced potential-subtracted mass m_{PS} [5]. From this mass definition we can obtain the $\overline{\text{MS}}$ -mass more accurately than from the pole mass scheme.

In the next section, we shall present the perturbative expansion of the correlator which is known up to next-to-next-to-leading order (NNLO). As was found in recent analyses of the Upsilon-system [6–10], the dominant theoretical contributions arise from the threshold expansion in the framework of non-relativistic QCD (NRQCD). These contributions will be derived in section 3. Afterwards, we shall shortly discuss the non-perturbative contributions and the phenomenological spectral function. In the numerical analysis, we shall first explain the method of analysis.

We will then obtain the pole mass and the $\overline{\text{MS}}$ -mass from an analysis in the pole mass and the PS-mass scheme respectively. The origin of different contributions to the error will be carefully investigated. We shall conclude with a summary and an outlook.

2. Perturbative expansion

The perturbative spectral function $R(v)$ can be expanded in powers of the strong coupling constant α_s ,

$$R^{Pt}(s) = R^{(0)}(s) + \frac{\alpha_s}{\pi} R^{(1)}(s) + \frac{\alpha_s^2}{\pi^2} R^{(2)}(s) + \dots$$

From this expression the corresponding moments \mathcal{M}_n can be calculated via the integral of eq. (2). The first two terms are known analytically and can for example be found in ref. [11]. $\Pi^{(2)}(s)$ is still not fully known analytically. However, the method of Padé-approximants has been exploited to calculate $\Pi^{(2)}$ numerically, using available results at high energies, analytical results for the first eight moments and the known threshold behaviour [12,13]. This information is sufficient to obtain a numerical approximation of $\Pi^{(2)}(s)$ in the full energy range.

The numerical stability of the results can be checked in different ways. By choosing different Padé-approximants or by selecting a smaller set of input data the results for the moments remain almost unchanged. Furthermore, some contributions to the spectral density like those from internal quark loops are known analytically and are in very good agreement with the numerical spectral density. The above are strong indicators that the numerically obtained spectral density comes very close to the exact spectral density.

3. Coulomb resummation

The perturbative expansion which contains terms up to the order $O(\alpha_s^2)$ is a good approximation for high velocities. However, as one approaches the threshold region, terms of the order $v(\alpha_s/v)^k$ become increasingly important. These terms can be obtained in the framework of NRQCD. The correlator is then expressed in

terms of a Greens function [8]:

$$\Pi(s) = \frac{N_c}{2M^2} \left(C_h(\alpha_s) G(k) + \frac{4k^2}{3M^2} G_C(k) \right),$$

where $k = \sqrt{M^2 - s/4}$ and M represents the pole mass. The constant $C_h(\alpha_s)$ is a perturbative coefficient which is needed for the matching between the full and the non-relativistic theory. It naturally depends on the hard scale. The Greens function is analytically known up to NNLO [8] and sums up terms of order α_s^n/v^{n-k} for $n \geq 0$ and $k = 1, 2, 3$. It is crucial for the analysis that the result depends on three scales. While the hard scale μ_{hard} is responsible for the hard perturbative processes, the soft scale μ_{soft} governs the expansion of the Greens function. Furthermore, the factorisation scale μ_{fac} separates the contributions of large and small momenta and plays the role of an infrared cutoff.

The Greens function contains two parts: the continuum and the poles above and below threshold respectively. We are interested in both contributions separately: first, the individual corrections can be analysed and their error estimated. Second, in our numerical analysis we will reconstruct the spectral density above threshold and we thus need the corresponding spectral density at low velocities. In principle, the expressions for the energies and decay widths of the poles have been calculated. However, in the actual case of the charm quark this expansion does not converge well. We will therefore choose a different method of evaluation. Since the results for the Greens function are known analytically, we can evaluate their contribution to the moments numerically by performing the derivatives. On the other hand, by using a dispersion relation, we can obtain the continuum from the imaginary part of the correlator. From the difference we can obtain the pole contributions:

$$\begin{aligned} \mathcal{M}_n^{Poles} &= \frac{12\pi^2}{n!} \left(4M^2 \frac{d}{ds} \right)^n \Pi(s) \Big|_{s=0} \\ &\quad - 12\pi (4M^2)^n \int_{4M^2}^{\infty} ds \frac{\text{Im} \Pi(s)}{s^{n+1}}. \end{aligned}$$

Since we will not evaluate the poles near threshold, but rather calculate their contributions to

the moments in a region where perturbation theory is expected to be valid, the convergence of the pole contributions is improved. Nevertheless, the poles will give the largest contribution to the theoretical moments and thus the dependence on the scales will remain relatively strong. The large corrections are partly due to the definition of the pole mass. These contributions can be reduced by using an intermediate mass definition. In this analysis we will use the potential-subtracted (PS) mass [5] where the potential below a separation scale μ_{sep} is subtracted:

$$\begin{aligned}\delta m(\mu_{sep}) &= -\frac{1}{2} \int_{|\mathbf{q}| < \mu_{sep}} \frac{d^3 q}{(2\pi)^3} V(q), \\ m_{PS}(\mu_{sep}) &= M - \delta m(\mu_{sep}).\end{aligned}$$

As will be seen in the numerical analysis, this mass definition leads to an improved scale dependence and a more precise determination of the $\overline{\text{MS}}$ -mass.

4. Condensate contributions

The non-perturbative effects on the vacuum correlator are parametrised by the condensates. The leading correction is the gluon condensate contribution which is known up to next-to-leading order [14]. Furthermore, the dimension 6 and 8 contributions have been calculated and will be included in our analysis [15,16]. It will turn out that the condensate contributions are suppressed when compared to former charmonium sum rule analyses and only have little influence on the mass. Besides an increase of the theoretical moments from the Coulomb contributions we will restrict the moments to $n \leq 7$ where the non-perturbative contributions are relatively small. Since we obtain a larger pole mass than the former analyses, the condensates, starting with a power of $1/M^4$, are suppressed further.

5. Phenomenological spectral function

Experimentally, the first six ψ -resonances have been observed. Since the widths of the poles are very small compared to the masses, the narrow-width approximation provides an excellent de-

scription of these states. To model the contributions above the 6th resonance, we use the assumption of quark-hadron-duality and integrate over the perturbative spectral density:

$$\frac{\mathcal{M}_n}{(4M^2)^n} = \frac{9\pi}{\alpha_{e.m.}^2 Q_c^2} \sum_{k=1}^6 \frac{\Gamma_k}{E_k^{2n+1}} + \int_{s_0}^{\infty} ds \frac{R^{Pt}(s)}{s^{n+1}}.$$

To estimate the continuum contribution we will use a threshold in the range of $3.6 \text{ GeV} \leq \sqrt{s_0} \leq 4.2 \text{ GeV}$ with a central value of $\sqrt{s_0} = 3.8 \text{ GeV}$. However, the most dominant phenomenological contributions come from the first two ψ -resonances resulting in a small influence of the continuum even for low values of n .

6. Numerical analysis

6.1. Analysing method

Besides the contributions from the poles of the Greens function and the condensates, the theoretical part of the correlator contains the spectral density above threshold. Now we will discuss the different parts of the spectral density. For high velocities the spectral density is well described by the perturbative expansion. However, as one approaches smaller values of v , the perturbative expansion breaks down. The resummed spectral density, on the other hand, gives a good description for low values of v , but becomes unreliable for high velocities. For these reasons, we will introduce a separation velocity $v_{sep} \approx 0.3$. Above v_{sep} we will use the perturbative spectral density. Below v_{sep} , we take the resummed spectral density adding the terms which are included in perturbation theory but not in resummation.

In fig. 1 we have displayed the different contributions. The dotted line represents the perturbative expansion in LO and NLO. The thin solid line also includes the NNLO. Whereas for high velocities the perturbative expansion is well convergent, the importance of the higher corrections increases for smaller v . The dashed line is the resummed spectral density and the thick solid line the reconstructed spectral density. For the charmonium system, there exists a range of intermediate values of v where neither the perturbative expansion nor the resummation can be trusted. Indeed, it can be clearly seen that the reconstructed

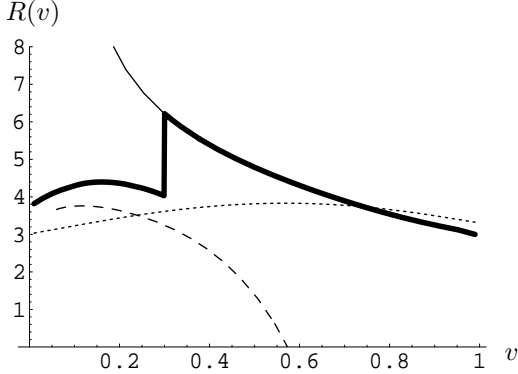


Figure 1. Thick solid line: reconstructed spectral density; Thin solid line: perturbative spectral density; dotted line: perturbation theory at NLO; dashed line: resummed spectral density.

spectral density shows a gap at the separation velocity. To estimate the error we have varied v_{sep} between 0.2 and 0.4. The analysis shows that though the introduction of the separation velocity stabilises the sum rules, the variation only has a minor influence on the mass.

6.2. Pole mass scheme

Since the perturbative corrections grow for large values of n , we will restrict our analysis to moments with $n \leq 7$. As our analysing method needs moments of $n \geq 3$ to reconstruct the spectral density, we will use $3 \leq n \leq 7$. As the central values for our scales we will choose

$$\begin{aligned} \mu_{soft} &= 1.2 \text{ GeV}, & \mu_{fac} &= 1.45 \text{ GeV}, \\ \mu_{hard} &= 1.7 \text{ GeV}. \end{aligned} \quad (3)$$

We have set the hard scale equal to the central value for the pole mass. For the soft scale, we would have liked to choose a somewhat smaller value, but the NNLO corrections get out of control for $\mu_{soft} \leq 1$ GeV. The factorisation scale lies between the two other scales. In this scheme the theoretical moments are dominated by the pole contributions. To estimate the error on the mass, we have varied the scales within reasonable ranges. The result is depicted in fig. 2. The thick

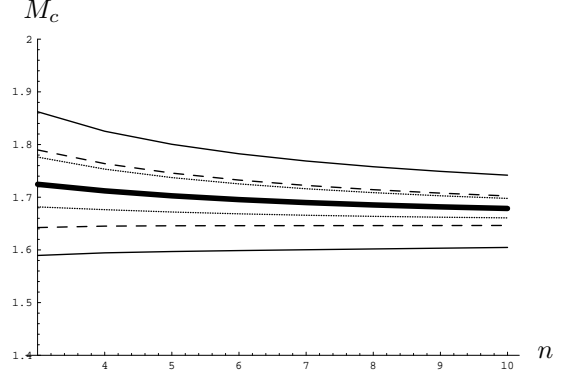


Figure 2. Thick solid line: central pole mass; thin solid lines: M_c for $\mu_{soft} = 1.05$ and 1.5 GeV; dashed lines: M_c for $\mu_{fac} = 1.2$ and 1.7 GeV; dotted lines: M_c for $\mu_{hard} = 1.4$ and 2.5 GeV.

solid line gives the central value for the charm mass of $M_c = 1.70$ GeV with the values of eq. (3). The error is dominated by the variation of the scales, we obtain

$$\begin{aligned} 1.05 \text{ GeV} \leq \mu_{soft} \leq 1.5 \text{ GeV} : \Delta M_c &= 100 \text{ MeV} \\ 1.2 \text{ GeV} \leq \mu_{fac} \leq 1.7 \text{ GeV} : \Delta M_c &= 50 \text{ MeV} \\ 1.4 \text{ GeV} \leq \mu_{hard} \leq 2.5 \text{ GeV} : \Delta M_c &= 40 \text{ MeV}. \end{aligned}$$

A significant uncertainty also comes from Λ_{QCD} . By choosing $\Lambda_{QCD} = 330 \pm 30$ MeV we get an

Table 1
Single contributions to the error of M .

Source	ΔM_c
Variation of μ_{soft}	100 MeV
Variation of μ_{fac}	50 MeV
Variation of μ_{hard}	40 MeV
Threshold s_0	10 MeV
Experimental error	15 MeV
Variation of v_{sep}	10 MeV
Variation of Λ_{QCD}	50 MeV
Total error	130 MeV

error of $\Delta M_c = 50$ MeV. The results are sum-

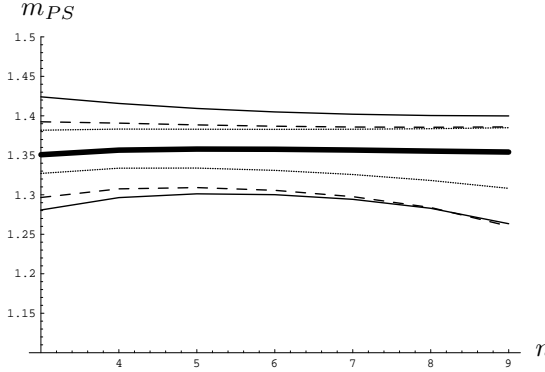


Figure 3. Thick solid line: central PS-mass; thin solid lines: m_{PS} for $\mu_{soft} = 1.05$ and 1.5 GeV; dashed lines: m_{PS} for $\mu_{fac} = 1.2$ and 1.7 GeV; dotted lines: m_{PS} for $\mu_{hard} = 1.4$ and 2.5 GeV.

marised in table 1. Adding the errors in quadrature we obtain the charm pole mass:

$$M_c = 1.70 \pm 0.13 \text{ GeV}. \quad (4)$$

Instead of deriving the $\overline{\text{MS}}$ -mass from the pole mass, in the following section we will use the PS-mass to obtain a more precise value for the $\overline{\text{MS}}$ -mass.

6.3. Potential-subtracted mass scheme

First, we have to choose a value for the separation scale μ_{sep} . This scale should be taken large enough to guarantee a perturbative relation to the $\overline{\text{MS}}$ -mass. On the other hand, it should be smaller than $M v$. Both conditions cannot be well fulfilled at the same time. As a compromise value we will choose $\mu_{sep} = 1.0 \pm 0.2$ GeV. In this scheme the pole contributions from the Greens function turn out to be smaller than in the pole mass scheme. The contributions from the condensates get more important here and we shall restrict our analysis to $n \leq 6$ where these corrections are under good control.

Using the same central values for the scales (3) we obtain $m_{PS}(\mu_{sep} = 1.0) = 1.35$ GeV and from this value a $\overline{\text{MS}}$ -mass of $m_c(m_c) = 1.23$ GeV. The introduction of the intermediate mass definition

leads to a reduced scale dependence:

$$\begin{aligned} 1.05 \text{ GeV} \leq \mu_{soft} \leq 1.5 \text{ GeV} : \Delta m_{PS} &= 60 \text{ MeV} \\ 1.2 \text{ GeV} \leq \mu_{fac} \leq 1.7 \text{ GeV} : \Delta m_{PS} &= 40 \text{ MeV} \\ 1.4 \text{ GeV} \leq \mu_{hard} \leq 2.5 \text{ GeV} : \Delta m_{PS} &= 30 \text{ MeV}. \end{aligned}$$

In table 2 we have listed the individual contrib-

Table 2
Single contributions to the error of m_{PS} and m_c .

Source	Δm_{PS}	Δm_c
Variation of μ_{soft}	60 MeV	50 MeV
Variation of μ_{fac}	40 MeV	40 MeV
Variation of μ_{hard}	30 MeV	30 MeV
Variation of μ_{sep}	30 MeV	30 MeV
Threshold s_0	30 MeV	30 MeV
Experimental error	10 MeV	10 MeV
Condensates	20 MeV	20 MeV
Variation of v_{sep}	10 MeV	10 MeV
Variation of Λ_{QCD}	10 MeV	20 MeV
Total error	90 MeV	90 MeV

butions to the error of m_{PS} and m_c . Finally, we obtain for the masses

$$\begin{aligned} m_{PS}(\mu_{sep} = 1.0) &= 1.35 \pm 0.09 \text{ GeV} \\ m_c(m_c) &= 1.23 \pm 0.09 \text{ GeV}. \end{aligned} \quad (5)$$

When we use the pole mass from eq. (4) and calculate the $\overline{\text{MS}}$ -mass using the three-loop relation between these masses [17,18], we obtain $m_c(m_c) = 1.20 \pm 0.17$ GeV. This value is in good agreement with eq. (5). This is not self-evident as the dominating pole contributions are reduced in the PS-scheme and the relative influence of the individual contributions is shifted.

7. Conclusions

The obtained value for the pole mass lies somewhat higher than in former sum rule analyses [19,20]. In [19] the authors used perturbation theory to NLO resulting in a value of $M_c = 1.46 \pm 0.07$ GeV. In the second investigation [20] the analysis has been performed in the $\overline{\text{MS}}$ -scheme with perturbation theory to NLO. Using the NLO relation to the pole mass the author obtains $m_c(m_c) = 1.26 \pm 0.05$ GeV and

$M_c = 1.42 \pm 0.03$ GeV. The author has also performed an analysis using resummation in LO with a value of $M_c = 1.45 \pm 0.07$ GeV. In our analysis the increased value of the pole mass is essentially due to large Coulomb contributions which have not been included in former analyses. As a consequence, the error becomes larger as well. In a recent analysis, the pole mass has been estimated from the charmonium ground state at NNLO [21]. Here the authors obtained a pole mass of $M_c = 1.88^{+0.22}_{-0.13}$ GeV. This value resulted from large corrections of the Coulomb potential to the ground state. During the last years, several lattice analyses obtained the following values for the $\overline{\text{MS}}$ -mass:

$$\begin{aligned} m_c(m_c) &= 1.59 \pm 0.28 \text{ GeV} [22], \\ m_c(m_c) &= 1.33 \pm 0.08 \text{ GeV} [23], \\ m_c(m_c) &= 1.73 \pm 0.26 \text{ GeV} [24], \\ m_c(m_c) &= 1.22 \pm 0.05 \text{ GeV} [25]. \end{aligned}$$

Whereas the results from [23,25] are in good agreement with this analysis, the investigations from [22] and [24] obtain higher masses. For the time-being, the results are not conclusive and future lattice calculations for the charm mass might be of interest. Since other methods reveal significant uncertainties in the determination of the quark masses, the sum rules remain one of the most precise methods to extract these fundamental quantities.

Acknowledgements M.Eidemüller would like to thank S. Narison for the invitation to this very “charm”ing and interesting conference.

REFERENCES

1. M.A. SHIFMAN, A.I. VAINSSTEIN AND V.I. ZAKHAROV, *Nucl. Phys.* **B 147** (1979) 385, *Nucl. Phys.* **B 147** (1979) 448.
2. L.J. REINDERS, H. RUBINSTEIN AND S. YAZAKI, *Phys. Rep.* **127** (1985) 1.
3. S. NARISON, QCD Spectral Sum Rules, World Scientific (1989).
4. M. BENEKE, *Phys. Rep.* **317** (1999) 1.
5. M. BENEKE, *Phys. Lett.* **B 434** (1998) 115.
6. J.H. KÜHN, A.A. PENIN AND A.A. PIVOVAROV, *Nucl. Phys.* **B 534** (1998) 356.
7. K. MELNIKOV AND A. YELKHOVSKY, *Phys. Rev.* **D 59** (1999) 114009.
8. A.A. PENIN AND A.A. PIVOVAROV, *Nucl. Phys.* **B 549** (1999) 217.
9. M. BENEKE AND A. SIGNER, *Phys. Lett.* **B 471** (1999) 233.
10. A.H. HOANG, *Phys. Rev.* **D 59** (1999) 014039.
11. M. JAMIN AND A. PICH, *Nucl. Phys.* **B 507** (1997) 334.
12. K.G. CHETYRKIN, J.H. KÜHN AND M. STEINHAUSER, *Nucl. Phys.* **B 482** (1996) 213.
13. K.G. CHETYRKIN, J.H. KÜHN AND M. STEINHAUSER, *Nucl. Phys.* **B 505** (1997) 40.
14. D.J. BROADHURST ET AL., *Phys. Lett.* **B 329** (1994) 103.
15. S.N. NIKOLAEV AND A.V. RADYUSHKIN, *Nucl. Phys.* **B 213** (1983) 285.
16. S.N. NIKOLAEV AND A.V. RADYUSHKIN, *Phys. Lett.* **B 124** (1983) 243.
17. K. MELNIKOV AND T. VAN RITBERGEN, *Phys. Lett.* **B 482** (2000) 99.
18. K.G. CHETYRKIN AND M. STEINHAUSER, *Nucl. Phys.* **B 573** (2000) 617.
19. C.A. DOMINGUEZ, G.R. GLUCKMAN AND N. PAVER, *Phys. Lett.* **B 333** (1994) 184.
20. S. NARISON, *Phys. Lett.* **B 341** (1994) 73, *Nucl. Phys.* **74** (Proc. Suppl.) (1999) 304.
21. A. PINEDA AND F.J. YNDURÁIN, *Phys. Rev.* **D 58** (1998) 094022.
22. C.R. ALLTON ET AL., *Nucl. Phys.* **B 431** (1994) 667.
23. A. KRONFELD, *Nucl. Phys.* **63** (Proc. Suppl.) (1998) 311.
24. V. GIMÉNEZ ET AL., *Nucl. Phys.* **B 540** (1999) 472.
25. A. BOCHKAREV AND P. DE FORCRAND, *Nucl. Phys.* **B 477** (1996) 489, *Nucl. Phys.* **53** (Proc. Suppl.) (1997) 305.